

# Supporting Information for [PB]Large-Scale Clustering of Tropical Precipitation and its Implications for the Radiation Budget across Timescales Can Large-Scale Clustering of Tropical Precipitation Be Used to Constrain Climate Sensitivity?

P. Blackberg<sup>1,2</sup>, M. S. Singh<sup>1,2</sup>

<sup>1</sup>School of Earth, Atmosphere, and Environment, Monash University, Victoria, Australia

<sup>2</sup>Centre of Excellence for the Weather of the 21st Century, Monash University, Victoria, Australia

## Contents of this file

1. Figures S1 to S8
2. Tables S1 to S2

---

Corresponding author: P. Blackberg, carlphiliposcar@gmail.com

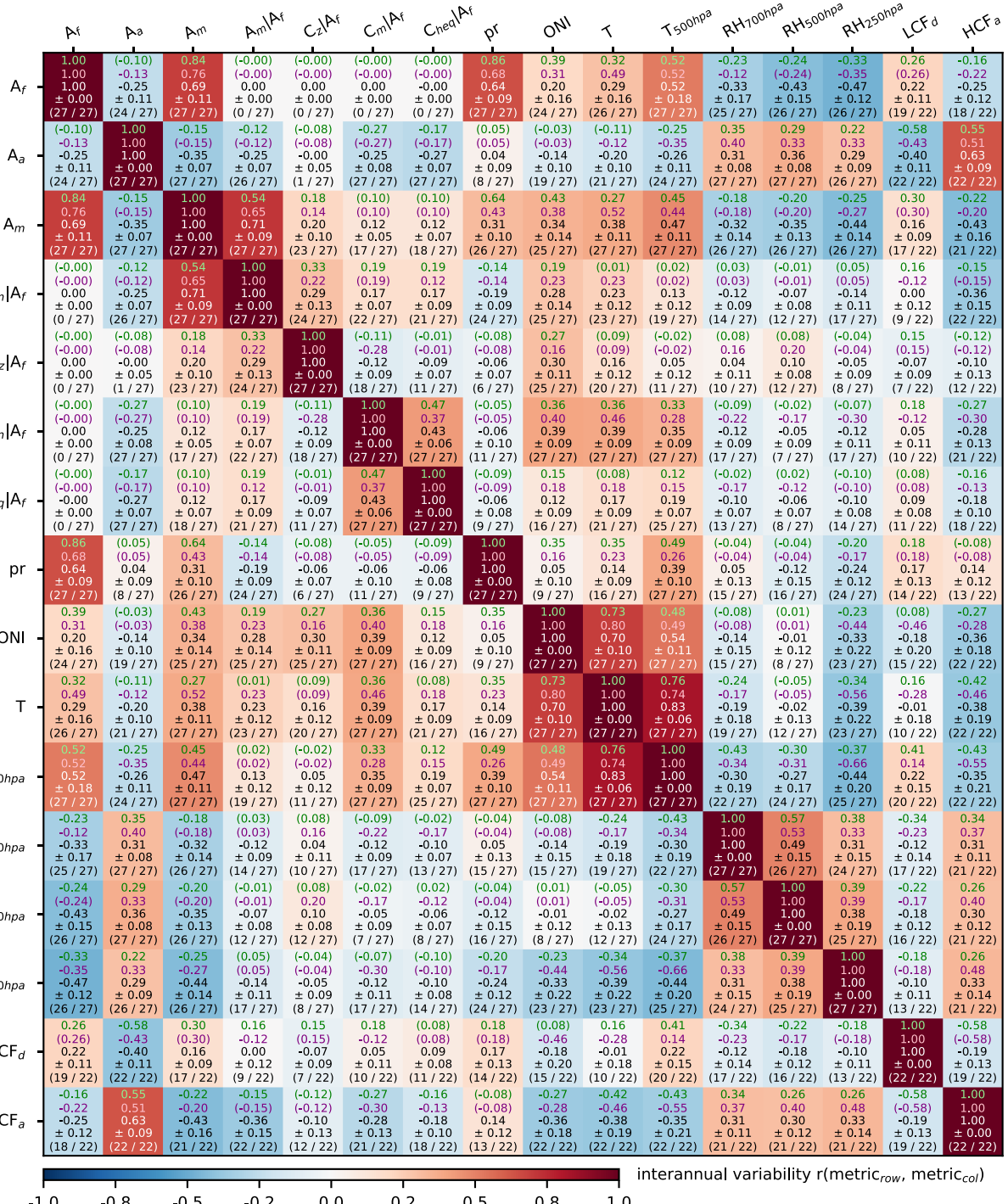


**Figure S1.** The  $ij$ 'th box show the correlation between metric in row  $i$  and column  $j$  for interannual variability in the CMIP ensemble. In each box, the top value shows ensemble-mean, the value below show standard deviation of correlations, and the fraction at the bottom shows what fraction of models have statistically significant correlations. Details of the metrics are given in Table S2.

January 5, 2026, 2:14pm

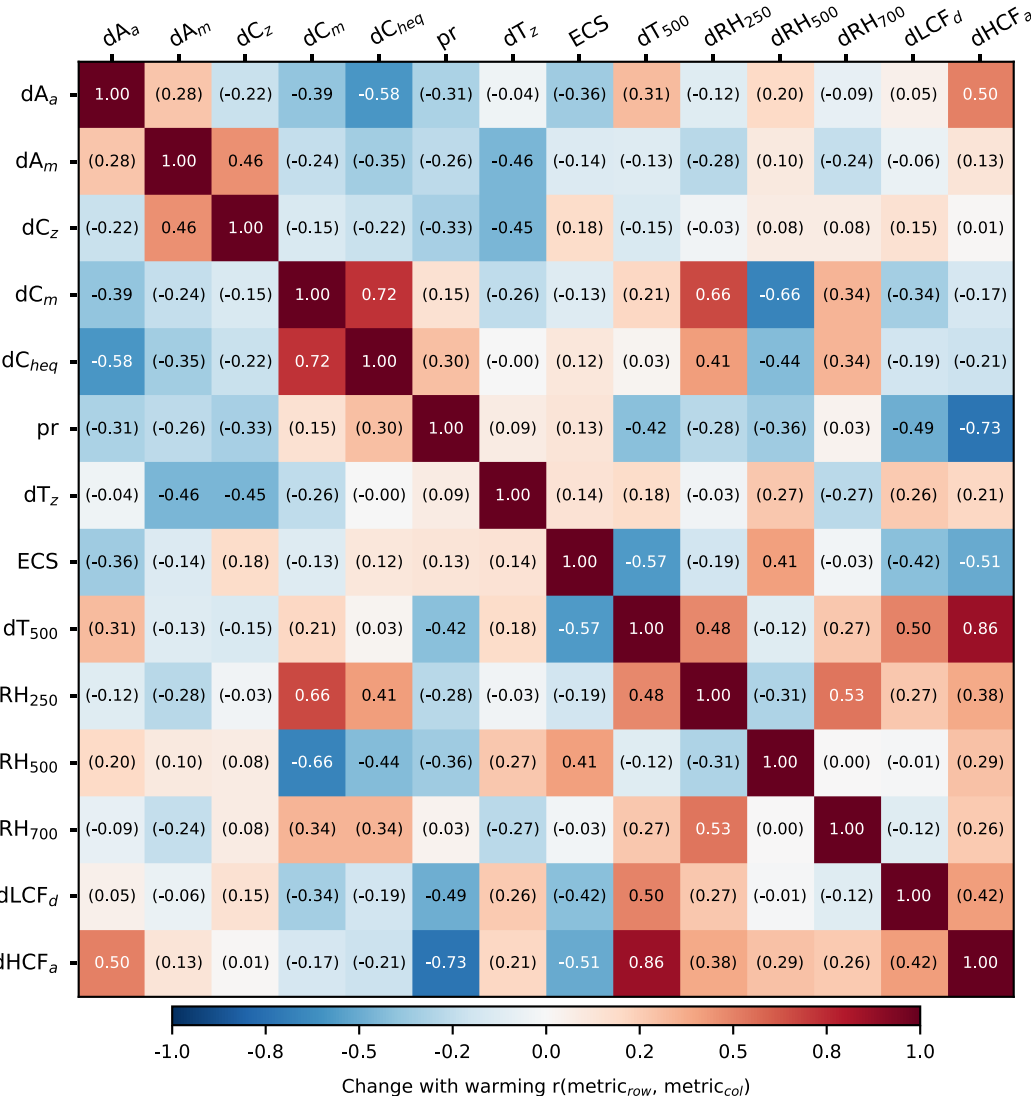


**Figure S2.** The ij'th box show the correlation between metric in row i and column j for interannual variability in observations. Numbers in brackets are not statistically significant form zero.

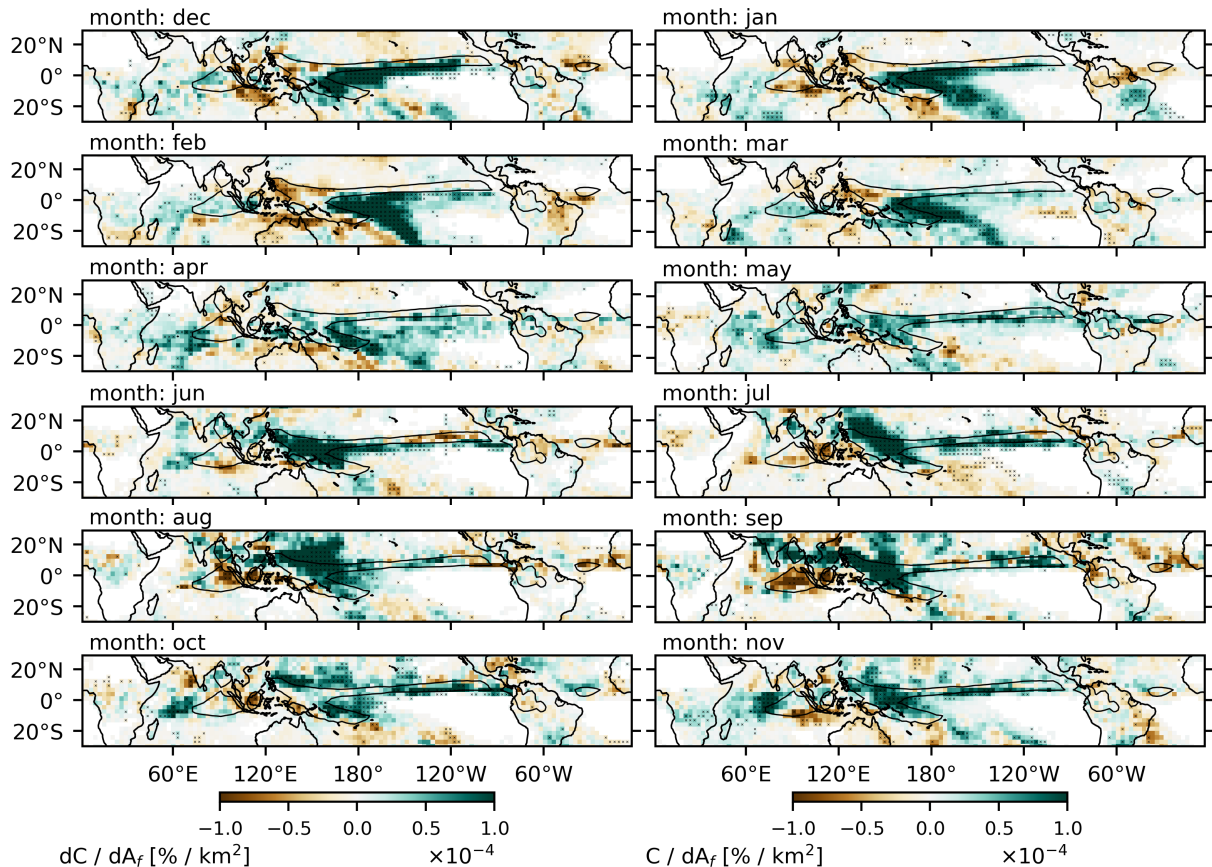


**Figure S3.** GPCP Frequency of occurrence of heavy precipitation,  $C$ , regressed onto the mean area of heavy precipitation features,  $A_m$ , for each month. Crosses indicate whether correlations are statistically significant.

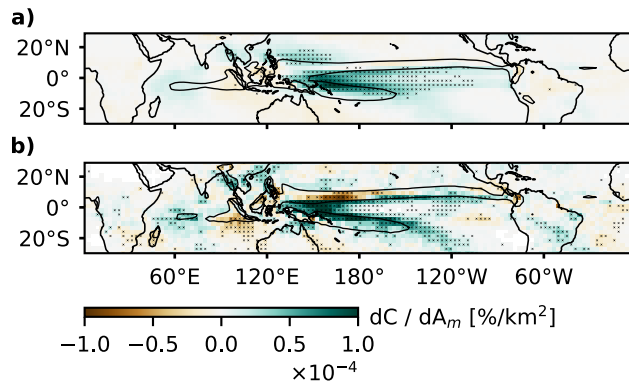


**Figure S4.** Frequency of occurrence of heavy precipitation,  $C$ , regressed onto the mean area of heavy precipitation features,  $A_m$ , in interannual variability for the CMIP ensemble-mean (a) and IFS\_9\_FESOM\_5 (b), and across the CMIP ensemble in climatological values (c). The contour shows the 90th percentile of the climatological  $C$  in (a-b) and the ensemble-mean 90th percentile of the climatological  $C$  in (c). Crosses indicate whether correlations are statistically significant.

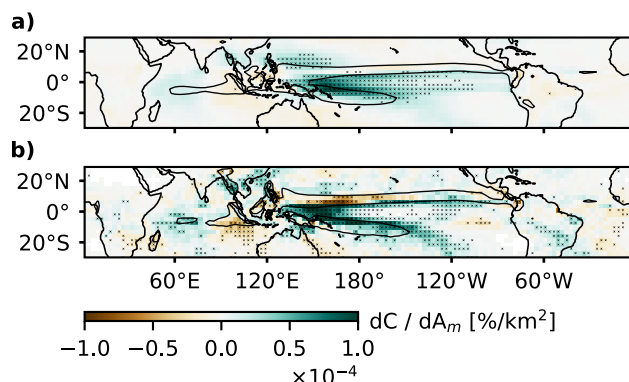


**Figure S5.** Frequency of occurrence of heavy precipitation,  $C$ , regressed onto the mean area of heavy precipitation features,  $A_m$ , in interannual variability for the CMIP ensemble-mean (a) and IFS\_9\_FESOM\_5 (b), and across the CMIP ensemble in climatological values (c). The contour shows the 90th percentile of the climatological  $C$  in (a-b) and the ensemble-mean 90th percentile of the climatological  $C$  in (c). Crosses indicate whether correlations are statistically significant.

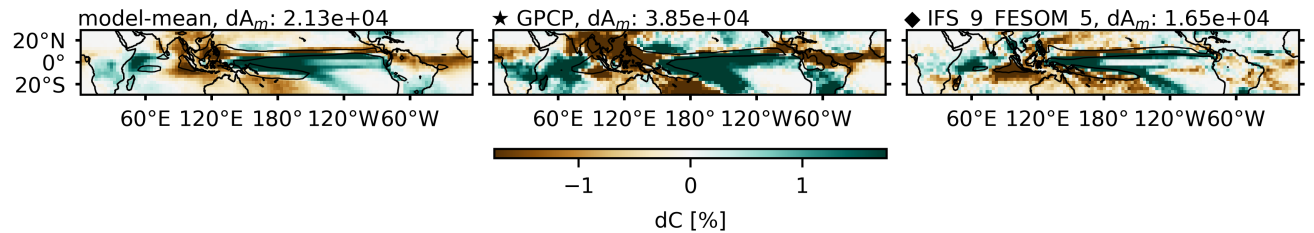


**Figure S6.** Difference in frequency of occurrence of heavy precipitation,  $C$ , during El Niño events and during all days in the CMIP ensemble-mean, in observations, and for the high-resolution model: IFS\_9\_FESOM\_5.

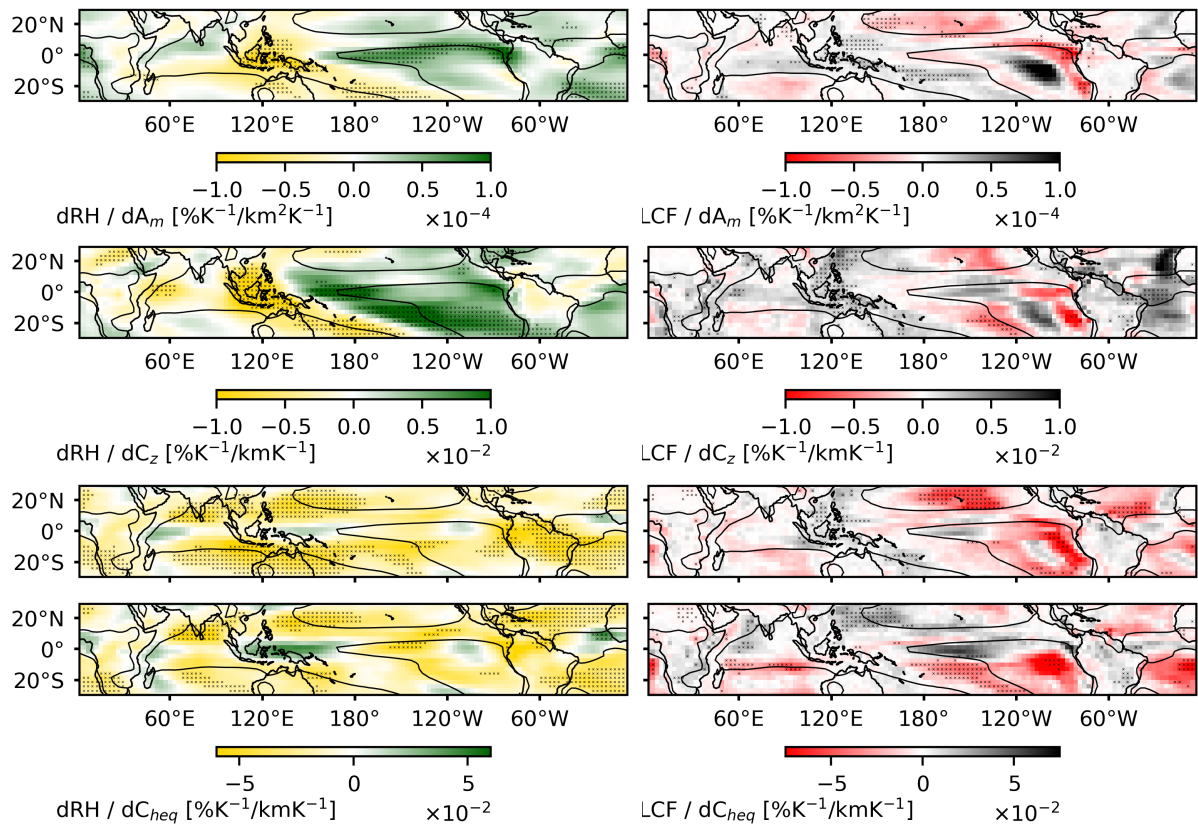


**Figure S7.** Change in relative humidity (RH, left) and low cloud fraction (LCF, right) regressed onto;  $A_m$  (a-b),  $C_z$  (c-d), and  $C_{heq}$  (e-f), per Kelvin warming across the CMIP ensemble.

**Table S1.** Models from the CMIP6 archive that were used in this study.

Institute	Model	Ensemble
INM	INM-CM5-0	r1i1p1f1
CCCR-IITM	IITM-ESM	r1i1p1f1
CAS	FGOALS-g3	r1i1p1f1
INM	INM-CM4-8	r1i1p1f1
MIROC	MIROC6	r1i1p1f1
MPI-M	MPI-ESM1-2-LR	r1i1p1f1
BCC	BCC-CSM2-MR	r1i1p1f1
NOAA-GFDL	GFDL-ESM4	r1i1p1f1
MIROC	MIROC-ES2L	r1i1p1f2
NorESM2-LM	NCC	r1i1p1f1
MRI	MRI-ESM2-0	r1i1p1f1
NOAA-GFDL	GFDL-CM4	r1i1p1f1
CMCC	CMCC-CM2-SR5	r1i1p1f1
CMCC	CMCC-ESM2	r1i1p1f1
NUIST	NESM3	r1i1p1f1
CSIRO	ACCESS-ESM1-5	r1i1p1f1
CNRM-CERFACS	CNRM-ESM2-1	r1i1p1f2
EC-Earth-Consortium	EC-Earth3	r1i1p1f1
CNRM-CERFACS	CNRM-CM6-1	r1i1p1f2
CNRM-CERFACS	CNRM-CM6-1-HR	r1i1p1f2
NIMS-KMA	KACE-1-0-G	r1i1p1f1
IPSL	IPSL-CM6A-LR	r1i1p1f1
CSIRO-ARCCSS	ACCESS-CM2	r1i1p1f1
AS-RCEC	TaiESM1	r1i1p1f1
NCAR	CESM2-WACCM	r1i1p1f1
CCCma	CanESM5	r1i1p1f1
MOHC	UKESM1-0-LL	r1i1p1f2

**Table S2.** Metrics used in this study.

Metric	description
$A_m$	Mean area of heavy precipitation features.
$A_f$	Total area of heavy precipitation features as a fraction of the tropical domain area.
$N$	Number of heavy precipitation features.
$C_z$	Mean distance of heavy precipitation points to the meridian given by the longitude 180°E.
$C_m$	Mean distance of heavy precipitation points to the equator.
$C_{heq}$	Mean distance of heavy precipitation points to the hydrological equator, where the hydrological equator is defined as the latitude of highest specific humidity at 700 hPa as a function of longitude for the associated month.
$T$	Tropical-mean 2 m air temperature.
$ONI$	Three-month rolling average SST anomaly in the Niño3.4 region (5°S- 5°N, 120°-170°W), relative to the full range of years used in the climatology.
$OLR$	Tropical-mean outgoing longwave radiation.
$LCF_d$	Tropical-mean low-cloud fraction, in regions where the monthly-mean vertical pressure velocity at 500 hPa is positive (in regions of descent).
$RH$	Tropical-mean relative humidity at 500 hPa.
$HCF_a$	Tropical-mean high-cloud fraction, in regions where the monthly-mean vertical pressure velocity at 500 hPa is negative (in regions of ascent).
$F_{pr10}$	Frequency of gridpoints exceeding 10 mm day <sup>-1</sup> .
$A_a$	Area covered by negative monthly-mean vertical pressure velocity at 500 hPa, as a fraction of the tropical domain area (area of ascent).
$\sigma(A_f)$	Standard deviation of total area fraction of heavy precipitation, $A_f$ .
$ECS$	Equilibrium Climate Sensitivity.